



University of Dundee

Xenobiotic CAR activators induce Dlk1-Dio3 locus non-coding RNA expression in mouse liver

Pouché , Lucie; Vitobello, Antonio; Römer, Michael ; Glogovac, Milica ; MacLeod, A. Kenneth; Ellinger-Ziegelbauer, Heidrun; Westphal, Magdalena ; Dubost, Valérie ; Stiehl, Daniel Philipp ; Dumotier, Bérengère ; Fekete, Alexander; Moulin, Pierre; Zell, Andreas; Schwarz, Michael; Moreno , Rita; Huang, Jeffrey T. J.; Elcombe, Cliff R.; Henderson, Colin J.; Wolf, C. Roland; Moggs, Jonathan G.; Terranova, Rémi

Published in:
Toxicological Sciences

DOI:
[10.1093/toxsci/kfx104](https://doi.org/10.1093/toxsci/kfx104)

Publication date:
2017

Document Version
Peer reviewed version

[Link to publication in Discovery Research Portal](#)

Citation for published version (APA):

Pouché , L., Vitobello, A., Römer, M., Glogovac, M., MacLeod, A. K., Ellinger-Ziegelbauer, H., ... Terranova, R. (2017). Xenobiotic CAR activators induce Dlk1-Dio3 locus non-coding RNA expression in mouse liver. *Toxicological Sciences*, 158(2), 367-378. <https://doi.org/10.1093/toxsci/kfx104>

General rights

Copyright and moral rights for the publications made accessible in Discovery Research Portal are retained by the authors and/or other copyright owners and it is a condition of accessing publications that users recognise and abide by the legal requirements associated with these rights.

- Users may download and print one copy of any publication from Discovery Research Portal for the purpose of private study or research.
- You may not further distribute the material or use it for any profit-making activity or commercial gain.
- You may freely distribute the URL identifying the publication in the public portal.

Xenobiotic CAR activators induce Dlk1-Dio3 locus non-coding RNA expression in mouse liver

Journal:	<i>Toxicological Sciences</i>
Manuscript ID	TOXSCI-16-0705.R1
Manuscript Type:	Research Article
Date Submitted by the Author:	n/a
Complete List of Authors:	<p>Pouche, Lucie; Novartis Institutes for Biomedical Research, Preclinical Safety, Translational Medicine Vitobello, Antonio; Novartis Institutes for Biomedical Research, Preclinical Safety, Translational Medicine Römer, Michael; University of Tübingen, Department of Computer Science Glogovac, Milica; Novartis Pharma AG, Novartis Business Services MacLeod, A. Kenneth; University of Dundee, Division of Cancer Research, Jacqui Wood Cancer Centre Ellinger-Ziegelbauer, Heidrun; Bayer Pharma AG, Westphal, Magdalena; Novartis Institutes for Biomedical Research, Preclinical Safety, Translational Medicine Dubost, Valerie; Novartis Institutes for Biomedical Research, Preclinical Safety, Translational Medicine Stiehl, Daniel; Novartis Institutes for Biomedical Research, Preclinical Safety, Translational Medicine Dumotier, Bérengère; Novartis Institutes for Biomedical Research, Preclinical Safety, Translational Medicine Fekete, Alexander; Novartis Institutes for Biomedical Research Moulin, Pierre; Novartis Institutes for Biomedical Research, Preclinical Safety, Translational Medicine Zell, Andreas; University of Tübingen, Center for Bioinformatics Schwarz, Michael; University of Tuebingen, Toxicology; Moreno, Rita; University of Dundee, Division of Cancer Research, Jacqui Wood Cancer Centre Huang, Jeffrey T. J. ; University of Dundee, Biomarker and Drug Analysis Core Facility, School of Medicine Elcombe, Clifford; CXR Biosciences, ; Henderson, Colin; University of Dundee, Cancer Research UK, Molecular Pharmacology Unit Wolf, C. Roland; University of Dundee, Cancer Research UK, Medical Research Institute Moggs, Jonathan; Novartis Pharma AG, Safety Profiling & Assessment, Investigative Toxicology Terranova, Remi; Novartis Institutes for Biomedical Research, Preclinical Safety, Translational Medicine</p>
Key Words:	Cancer Risk Assessment, Constitutive Androstane Receptor (CAR), biomarkers < Safety Evaluation, non-genotoxic < Carcinogenesis, Dlk1-

1
2
3
4
5
6
7
8
9
10
11
12
13
14
15
16
17
18
19
20
21
22
23
24
25
26
27
28
29
30
31
32
33
34
35
36
37
38
39
40
41
42
43
44
45
46
47
48
49
50
51
52
53
54
55
56
57
58
59
60

	Dio3 cluster long non-coding RNAs

SCHOLARONE™
Manuscripts

Xenobiotic CAR activators induce Dlk1-Dio3 locus non-coding RNA expression in mouse liver

Lucie Pouché*, Antonio Vitobello*, Michael Römer¹, Milica Glogovac, A. Kenneth MacLeod, Heidrun Ellinger-Ziegelbauer¹, Magdalena Westphal, Valérie Dubost, Daniel Philipp Stiehl, Bérengère Dumotier, Alexander Fekete, Pierre Moulin, Andreas Zell¹, Michael Schwarz¹, Rita Moreno, Jeffrey T. J. Huang, Cliff R. Elcombe¹, Colin J. Henderson¹, C. Roland Wolf¹, Jonathan G. Moggs¹, Rémi Terranova**

Author affiliations:

Lucie Pouché: **contributed equally to this work*, Preclinical Safety, Translational Medicine, Novartis Institutes for Biomedical Research, CH-4057 Basel, Switzerland, pouche.lucie@gmail.com

Antonio Vitobello: **contributed equally to this work*, Preclinical Safety, Translational Medicine, Novartis Institutes for Biomedical Research, CH-4057 Basel, Switzerland, antonio.vitobello@novartis.com

Milica Glogovac: Novartis Business Services, Novartis Pharma, CH-4057 Basel, Switzerland, milica.glogovac@novartis.com

Michael Römer: Department of Computer Science, University of Tübingen, Sand 1, 72076 Tübingen, Germany, michael.roemer@uni-tuebingen.de

1
2
3 A. Kenneth MacLeod: Division of Cancer Research, Jacqui Wood Cancer Centre,
4 University of Dundee, James Arrott Drive, Ninewells Hospital And Medical School,
5 Dundee, DD1 9SY, United Kingdom, K.A.Z.MacLeod@dundee.ac.uk
6
7
8

9
10 Heidrun Ellinger-Ziegelbauer: Investigational Toxicology, GDD-GED-Toxicology,
11 Bayer Pharma AG, 42096 Wuppertal, Germany, heidrun.ellinger-
12 ziegelbauer@bayer.com
13
14
15

16
17 Magdalena Westphal: Preclinical Safety, Translational Medicine, Novartis Institutes
18 for Biomedical Research, CH-4057 Basel, Switzerland,
19 magdalena.westphal@novartis.com
20
21
22

23
24 Valérie Dubost: Preclinical Safety, Translational Medicine, Novartis Institutes for
25 Biomedical Research, CH-4057 Basel, Switzerland,
26 valerie.dubost@novartis.com
27
28
29

30
31 Daniel Philipp Stiehl: Preclinical Safety, Translational Medicine, Novartis Institutes for
32 Biomedical Research, CH-4057 Basel, Switzerland, daniel.stiehl@novartis.com
33
34
35

36
37 Bérengère Dumotier: Preclinical Safety, Translational Medicine, Novartis Institutes for
38 Biomedical Research, CH-4057 Basel, Switzerland,
39 berengere.dumotier@novartis.com
40
41
42

43
44 Alexander Fekete: Preclinical Safety, Translational Medicine, Novartis Institutes for
45 Biomedical Research, Inc. 250 Massachusetts Avenue, Cambridge, MA 02139,
46 United States, alexander.fekete@novartis.com
47
48
49

50
51 Pierre Moulin: Preclinical Safety, Translational Medicine, Novartis Institutes for
52 Biomedical Research, CH-4057 Basel, Switzerland, pierre.moulin@novartis.com
53
54
55

1
2
3 Andreas Zell: Department of Computer Science, University of Tübingen, Sand 1,
4
5 72076 Tübingen, Germany, andreas.zell@uni-tuebingen.de
6
7

8 Michael Schwarz: Department of Toxicology, University of Tübingen, Wilhelmstr. 56,
9
10 72074 Tübingen, Germany, michael.schwarz@uni-tuebingen.de
11
12

13 Rita Moreno: Division of Cancer Research, Jacqui Wood Cancer Centre, University
14
15 of Dundee, James Arrott Drive, Ninewells Hospital And Medical School, Dundee,
16
17 DD1 9SY, United Kingdom, ritadorta@gmail.com
18
19

20 Jeffrey T. J. Huang: Biomarker and Drug Analysis Core Facility, School of Medicine,
21
22 University of Dundee, Jacqui Wood Cancer Centre, Ninewells Hospital, Dundee, DD1
23
24 9SY, United Kingdom, j.t.j.huang@dundee.ac.uk
25
26
27

28 Cliff R. Elcombe: CXR Biosciences Ltd., 2 James Lindsay Place, Dundee
29
30 Technopole, Dundee Scotland DD1 5JJ, cliffelcombe@cxrbiosciences.com
31
32
33

34 Colin J. Henderson: Division of Cancer Research, Jacqui Wood Cancer Centre,
35
36 University of Dundee, James Arrott Drive, Ninewells Hospital And Medical School,
37
38 Dundee, DD1 9SY Medical Research Institute, University of Dundee, Dundee, United
39
40 Kingdom, c.j.henderson@dundee.ac.uk
41
42
43

44 C. Roland Wolf: Division of Cancer Research, Jacqui Wood Cancer Centre,
45
46 University of Dundee, James Arrott Drive, Ninewells Hospital And Medical School,
47
48 Dundee, DD1 9SY Medical Research Institute, University of Dundee, Dundee, United
49
50 Kingdom, c.r.wolf@dundee.ac.uk
51
52
53

54 Jonathan G. Moggs: Preclinical Safety, Translational Medicine, Novartis Institutes for
55
56 Biomedical Research, CH-4057 Basel, Switzerland, jonathan.moggs@novartis.com
57
58
59
60

1
2
3 Rémi Terranova: **corresponding author, Preclinical Safety, Translational Medicine,
4
5 Novartis Institutes for Biomedical Research, CH-4057 Basel, Switzerland,
6
7 remi.terranova@novartis.com
8
9
10
11
12

13 ¹MARCAR consortium member
14

15 *Contributed equally to the work
16

17 **Corresponding author
18
19
20
21

22 **Keywords:** *Dlk1-Dio3* cluster, non-coding RNAs, Constitutive Androstane Receptor
23
24 (CAR), Non-genotoxic Carcinogenesis (NGC), Cancer Risk Assessment,
25
26 Phenobarbital, Chlordane
27
28
29
30
31
32
33
34
35
36
37
38
39
40
41
42
43
44
45
46
47
48
49
50
51
52
53
54
55
56
57
58
59
60

Abstract

Derisking xenobiotic-induced non-genotoxic carcinogenesis (NGC) represents a significant challenge during the safety assessment of chemicals and therapeutic drugs. The identification of robust mechanism-based NGC biomarkers has the potential to enhance cancer hazard identification. We previously demonstrated Constitutive Androstane Receptor (CAR) and WNT signaling-dependent up-regulation of the pluripotency associated *Dlk1-Dio3* imprinted gene cluster non-coding RNAs (ncRNAs) in the liver of mice treated with tumor-promoting doses of phenobarbital (PB). Here, we have compared phenotypic, transcriptional and proteomic data from wild-type, CAR/PXR double knock-out and CAR/PXR double humanized mice treated with either PB or chlordane, and show that hepatic *Dlk1-Dio3* locus long ncRNAs are upregulated in a CAR/PXR-dependent manner by two structurally distinct CAR activators. We further explored the specificity of *Dlk1-Dio3* locus ncRNAs as hepatic NGC biomarkers in mice treated with additional compounds working through distinct NGC modes of action. We propose that up-regulation of *Dlk1-Dio3* cluster ncRNAs can serve as an early biomarker for CAR activator-induced non-genotoxic hepatocarcinogenesis and thus may contribute to mechanism-based assessments of carcinogenicity risk for chemicals and novel therapeutics.

1. Introduction

Assessing the risk for xenobiotic-induced non-genotoxic carcinogenesis (NGC) is a major challenge for safety scientists. This is exemplified by the broad range of cancer hazard identification strategies that are selectively deployed during the preclinical development of novel therapeutics based on their modality, mode of action, disease indication, and phase of development (Moggs et al. 2016). Derisking drug-induced carcinogenicity would benefit from the development of reliable mechanism-based biomarkers that enable early cancer hazard identification and also enhance mechanistic insight for positive tumor findings in life-time rodent carcinogenicity studies.

The liver is a major target organ for xenobiotic-induced NGC. We have used Phenobarbital (PB), an anticonvulsant commonly used for treatment of epilepsy and other seizures, as a model compound to study mechanisms underlying liver NGC mechanisms. PB indirectly activates CAR through molecular pathways that have been reported to include the inhibition of epidermal growth factor receptor signaling (Mutoh et al. 2013). PB-mediated liver tumor promotion in mice is dependent on CAR and β -catenin (Huang et al. 2005; Rignall et al. 2011; Yamamoto et al. 2004). Furthermore, β -catenin harbours activating mutations in most CAR-dependent mouse liver tumors (Unterberger et al. 2014; Aydinlik et al. 2001). Through integrated molecular profiling, we previously uncovered an early, progressive and long-lasting, CAR- and β -catenin-dependent up-regulation of the *Dlk1-Dio3* imprinted cluster ncRNAs in perivenous hepatocytes of mice treated with tumor-promoting doses of PB (Lempiainen et al. 2013; Luisier et al. 2014). Several groups have reported a potential role for *Dlk1-Dio3* derived non-coding transcripts in stem cell pluripotency (Liu et al. 2010; Stadtfeld and Hochedlinger 2010). The overexpression of the human

1
2
3 *Dlk1-Dio3* miRNA cluster was also positively correlated with expression of
4 hepatocellular carcinoma (HCC) stem cells markers and was also associated with
5 poor survival rate in HCC patients (Luk et al. 2011). Many of the *Dlk1-Dio3* cluster
6 miRNAs are differentially expressed in hepatocellular carcinomas (Benetatos,
7 Vartholomatos, and Hatzimichael 2014; Cui et al. 2015; Xu et al. 2013; Yin et al.
8 2013). Together, these observations highlight a pathophysiological role for *Dlk1-Dio3*
9 ncRNA dysregulation in liver cancer and support their functional relevance as early
10 NGC biomarkers.
11
12
13
14
15
16
17
18
19

20
21 Xenobiotic-induced activation of CAR and/or Pregnane X receptor (PXR) triggers an
22 immediate activation of specific subsets of cytochrome P450 (CYP)-encoding genes,
23 including the *Cyp2b* and *Cyp2c* family isoforms. CAR and PXR trans-activate a large
24 battery of genes involved in phase I oxidation and phase II conjugation pathways that
25 contribute to xenobiotic metabolism. PXR and CAR receptors have overlapping
26 functions in the regulation of xenobiotic metabolism genes such as *Cyp3a*, whilst
27 CAR- and PXR-specific target genes have also been identified (Cui and Klaassen
28 2016; Wei et al. 2002). Chronic CAR activation by PB or other (in)direct activators is
29 associated with hepatocellular carcinoma, liver injury, glucose metabolism and
30 cholesterol homeostasis (Kobayashi et al. 2015). It was previously proposed that
31 monitoring of P450-encoding genes such as *Cyp2b10*, one of the most strongly
32 regulated CAR targets, could provide a robust surrogate biomarker of CAR activation
33 in drug-induced mouse liver tumors (Hoflack et al. 2012).
34
35
36
37
38
39
40
41
42
43
44
45
46
47
48
49

50
51 To explore further the NGC-specificity and CAR-activation dependence of xenobiotic-
52 induced liver *Dlk1-Dio3* long non-coding RNAs (*lncRNAs*) activation, we compared
53 phenotypic, transcriptional and proteomic data from wild-type and CAR/PXR
54 transgenic C57BL/6 mouse models following *in vivo* treatment with PB and the
55
56
57
58
59
60

1
2
3 pesticide-derived CAR-activator chlordane (Malarkey 1995; Moser and Smart 1989;
4
5 Ruch et al. 1990). We further investigated selected transcriptional profiles from
6
7 mouse liver samples exposed to additional NGC compounds that work through
8
9 different modes of action (MoA), and show that up-regulation of hepatic *Dlk1-Dio3*
10
11 cluster non-coding RNAs represents a common feature of CAR-activating
12
13 compounds. Our study highlights *Dlk1-Dio3* imprinted cluster lncRNAs as potential
14
15 CAR activator-specific hepatic biomarkers that warrant further evaluation as tools for
16
17 mechanism-based safety assessment of xenobiotic-induced liver non-genotoxic
18
19 carcinogenesis.
20
21
22
23
24
25
26
27
28
29
30
31
32
33
34
35
36
37
38
39
40
41
42
43
44
45
46
47
48
49
50
51
52
53
54
55
56
57
58
59
60

2. Material and methods

2.1. Ethics statement

In vivo mouse studies were performed either according to the Institutional Guidelines of the University of Tübingen (Rignall et al. 2011) or in conformity with the Swiss Animal Welfare Law -Animal Licenses No. 2345 by “Kantonales Veterinäramt Basel-Stadt” [Cantonal Veterinary Office, Basel] and No. 5041 by “Kantonales Veterinäramt Baselland” [Cantonal Veterinary Office, Basel Land].

2.2. Animal husbandry and dosing

For the chlordane *in vivo* study, eight to eleven week-old male CAR^h-PXR^h, CAR^{KO}-PXR^{KO} and wild-type C57BL/6 mice were used (Taconic, Germany). Animals were randomly allocated in groups of 5 per treatment and time point. Mice were checked daily for activity and behavior and administered with chlordane (Sigma-Aldrich [St Louis, MO] #PS75, 8 mg/kg/day), or corn oil (vehicle) by oral gavage – treatment doses were selected based on (Ross et al. 2010; Barrass et al. 1993). After 28 days (t=28) of treatment, the compound was withdrawn and the recovery group animals kept for a further 28 days for reversibility assessment (t=56). At sacrifice, on day 29 (2 hrs post-dose) and 57 (recovery period), blood was sampled for pharmacokinetics (PK) analysis and hepatic lobes were collected and either frozen in liquid nitrogen and stored at -80°C for subsequent analyses or fixed in neutral phosphate-buffered formalin and paraffin-embedded (FFPE). To ensure sample homogeneity for different molecular profiling methods, frozen liver samples were reduced to powder with Covaris Cryoprep system (Covaris Inc., Woburn, MA) and aliquoted on dry ice. For the Phenobarbital study comparison, samples from the *in vivo* study using C57BL/6

9

1
2
3 Wild-type (WT), CAR/PXR double knockout (CAR^{KO}-PXR^{KO}) and humanized
4 CAR/PXR (CAR^h-PXR^h) mice chronically exposed for 28 days (t=28), 91 days (t=91)
5 or 91 days followed by 28 days of recovery (t=119) from (Luisier et al. 2014) were
6 analyzed. Additional justification on compounds dose selection is available in
7 Supplementary Material and Methods.
8
9

10 11 12 13 14 **2.3. Cross-compound data mining, Affymetrix labeling, GeneChip** 15 **processing and gene expression analysis** 16

17
18 We performed data mining of *in vivo* gene expression profiles produced by the
19 MARCAR consortium (<http://www.imi-marcar.eu/>) encompassing six well-known liver
20 NGC compounds: Phenobarbital (PB), Pirinixic acid (Wy), Piperonyl Butoxide (PBO),
21 1,4-dichlorobenzene (DCB), Cyproterone acetate (CPA), and methapyrilene (Mpy).
22 Pioglitazone (Pio) was used as a non-hepatocarcinogen compound and CITCO as a
23 human specific CAR activator. Data sets of Wy, PBO, DCB, CPA, MPY, PB, CITCO
24 and Pio studies were publically released and available at NCBI's GEO (GSE68364
25 and GSE60684). Affymetrix labeling and GeneChip (Mouse Genome 430 2.0 Array)
26 processing were conducted as described in (Lempiainen et al. 2013). Heatmaps were
27 built using TIBCO Spotfire®. GeneChip and qPCR expression data analyses were
28 described in Supplementary Materials and Methods.
29
30
31
32
33
34
35
36
37
38
39
40
41
42
43
44

45 **2.4. RT-qPCR analyses**

46
47 RNA isolation and quantitative RT-PCR analyses were performed as previously
48 described (Lempiainen et al. 2013) and are detailed in Supplementary Materials and
49 Methods. All expression analyses are based on qPCR, primer sequences are
50 provided in (Lempiainen et al. 2013) and Supplementary Materials and Methods.
51
52
53
54
55
56
57
58
59
60

1
2
3 versus untreated (vehicle) qPCR signal differences (n=5/group) were tested using
4
5 unpaired t-tests with Welch's correction for unequal variance.
6
7

8 **2.5. Proteomic analysis**

9
10 Sample preparation, data acquisition and analysis by targeted high resolution single
11 ion monitoring (tHR/SIM) *in vivo* 'stable isotope labelling by amino acids in cell
12 culture' (SILAC) using a pathway-enhanced internal standard was carried out as
13 described previously (MacLeod et al. 2015) (Supplementary Material and Methods).
14
15 For generation of the hierarchical clustering heatmaps, Xcalibur files were processed
16 using MaxQuant, version 1.4.1.2, (Cox and Mann 2008) and the integrated
17 Andromeda search engine with the Uniprot Mus musculus (taxID: 10090) reference
18 proteome set (44,455 entries, downloaded 03.12.14). Cysteine carbamidomethylation
19 was set as a fixed modification, with N-terminal acetylation and methionine oxidation
20 as variable modifications. The protein false discovery rate was set to 1%, minimum
21 peptide length was 7 and a maximum of 2 miscleavages was allowed. Data were
22 processed in Perseus (version 1.5.1.6). For each control/xenobiotic comparison, only
23 proteins with ≥ 3 valid values were retained. Data were analyzed using GraphPad
24 Prism 7.0. Statistical significance of treated versus untreated (vehicle) signal
25 differences were tested using multiple unpaired t-tests on log₂ transformed data. The
26 p-values were adjusted using Holm-Sidak method, with alpha = 0.05.
27
28
29
30
31
32
33
34
35
36
37
38
39
40
41
42
43
44
45

46 For proteomics heatmap generation, individual animal data were normalised to the
47 mean of the control group, log₂-transformed and missing values imputed from normal
48 distribution. Clustering was generated in R using the RStudio interface with the gplots
49 and RColorBrewer packages.
50
51
52
53
54

55 **2.6. In situ hybridization (ISH) and Immunohistochemistry (IHC)**

1
2
3 *Meg3* *in situ* hybridization (ISH) and glutamine synthetase (GS)
4 immunohistochemistry (IHC) were conducted on liver samples of chlordane- and PB-
5 treated animals as previously described (Lempiainen et al. 2013), detailed in
6
7 Supplementary Materials and Methods.
8
9
10
11
12
13
14
15
16
17
18
19
20
21
22
23
24
25
26
27
28
29
30
31
32
33
34
35
36
37
38
39
40
41
42
43
44
45
46
47
48
49
50
51
52
53
54
55
56
57
58
59
60

3. Results

3.1. Comparable liver phenotypic and histopathologic responses following 28 days *in vivo* PB and chlordane treatment of mice.

We previously showed that the *Dlk1-Dio3* transcriptional response mediated by PB is CAR-dependent (Lempiainen et al. 2013; Luisier et al. 2014). In order to further evaluate the specificity of this candidate NGC biomarker for CAR activators, we compared the effects of PB and chlordane in the liver of WT, CAR/PXR double knockout (CAR^{KO}-PXR^{KO}) and double humanized (CAR^h-PXR^h) C57BL/6 animals after 28 days (t=28) treatment with either compound (**Fig. 1A**). Akin to PB, chlordane is a NGC compound which induces hepatomegaly characterized by hypertrophy and hyperplasia and acts through robust CAR activation (Ross et al. 2010; Barrass et al. 1993; Malarkey 1995; Whysner et al. 1998).

No significant body weight differences were observed comparing 28 days PB and chlordane treated samples (**Table 1**). Microscopically, similar histopathological changes were observed in liver, characterized by moderate centrilobular hepatocellular hypertrophy in WT after 28 days with both treatments. Centrilobular hepatocytes showed cytoplasmic changes with an eosinophilic and/or granular basophilic cytoplasm in chlordane treated samples (data not shown). Comparable, moderate to marked, changes were also made in CAR^h-PXR^h animals. No morphological alterations were present in CAR^{KO}-PXR^{KO} mice with either compound. Following recovery, centrilobular hypertrophy and cytoplasmic changes were still present in both WT and CAR^h-PXR^h mice in chlordane- and PB-treated samples, although less pronounced in humanized groups.

1
2
3 Interestingly, plasma concentration of chlordane-treated samples showed
4 appreciable compound levels after 28 days of recovery (t=56, 1 µg/mL in WT
5 animals) consistent with chlordane's long half-life (Zucker 1985). PB on the other
6 hand was undetectable after 28 days recovery (t=56) (**Table 1**). Overall, the liver
7 histopathological changes induced by chlordane are CAR/PXR-activation dependent
8 and similar to those induced by PB.
9
10
11
12
13
14
15
16
17

18 **3.2. Both chlordane and PB induce *Dlk1-Dio3* lncRNA up-regulation in** 19 **perivenous hepatocytes** 20 21 22 23

24 We next investigated the transcriptional response of *Dlk1-Dio3* lncRNAs in chlordane
25 and PB treated mice. Using RT-qPCR, we profiled the expression of both coding and
26 long non-coding transcripts throughout the *Dlk1-Dio3* cluster in 28-day PB and
27 chlordane liver study samples (t=28) (**Fig. 1A**). The imprinted *Dlk1-Dio3* locus
28 contains three protein coding genes (*Dlk1*, *Dio3* and *Rtl1*) expressed from the
29 paternally inherited allele, and several maternal-of-origin lncRNAs (*Meg3*, *anti-Rtl1*,
30 *Rian* and *Mirg*) (Benetatos, Vartholomatos, and Hatzimichael 2014) (**Fig. 1B**).
31 Strikingly, PB and chlordane triggered comparable transcriptional activation of *Meg3*,
32 *anti-Rtl1*, *Rian* and *Mirg* lncRNAs in wild-type animals (**Fig. 1C**) with no detectable
33 activation of the coding genes *Dlk1* and *Dio3*. Consistent with long half-life of
34 chlordane (**Table 1**), increased levels of *Meg3*, *anti-Rtl1*, *Mirg* and *Cyp2b10*
35 expression were observed in chlordane (but not PB) recovery group animals (t=56
36 and t=119 respectively) (**Supplementary Fig.S1**).
37
38
39
40
41
42
43
44
45
46
47
48
49
50
51
52

53 We had previously shown that *Meg3* expression occurs within a specific subset of
54 perivenous hepatocytes expressing glutamine synthetase (GS) following PB
55 treatment (Lempiainen et al. 2013). The *Glu1* gene encoding for the GS protein is a
56
57
58
59
60

1
2
3 target regulated positively by the WNT signaling pathway and is also expressed in
4
5 PB-promoted tumors (Loeppen et al. 2002). Immunohistochemistry (IHC) and *in situ*
6
7 hybridization (ISH) directed against GS and *Meg3* respectively showed similar *Meg3*
8
9 lncRNA distribution and no apparent change in GS expression levels with either
10
11 compound in 28-day treated samples (**Fig. 1D**), altogether consistent with CAR- and
12
13 β -catenin dependence of the *Dlk1-Dio3* lncRNAs activation.
14
15
16
17
18
19

20 **3.3. Differential liver *Dlk1-Dio3* lncRNA activation in humanized** 21 **CAR/PXR mice following PB versus chlordane exposure**

22
23
24 CAR and PXR double knockouts (CAR^{KO}-PXR^{KO}) and double humanized CAR and
25
26 PXR (CAR^h-PXR^h) mouse models were used to examine CAR/PXR dependencies
27
28 and potential species differences in receptor-dependent responses to chlordane (**Fig.**
29
30 **1A**). As described previously (Luisier et al. 2014), PB led to comparable activation of
31
32 *Dlk1-Dio3* lncRNAs in WT and humanized mice models (approx. 20 fold increase
33
34 over vehicle controls - compare **Fig. 2A** and **Fig. 1C**, red bars). In contrast, while
35
36 chlordane treatment led to over 10 fold induction of *Dlk1-Dio3* lncRNAs in WT
37
38 animals (**Fig. 1C**, orange bars), the cluster was minimally induced (approx. 2.5 fold
39
40 induction over control) upon chlordane treatment of CAR^h-PXR^h animals (**Fig.**
41
42 **2A**). Consistently, lower levels of *Cyp2b10* (**Fig. 2C**) were also detected in chlordane-
43
44 treated CAR^h-PXR^h mice expressing hCAR (**Fig. 2D**) as compared to WT animals.
45
46
47
48
49
50
51
52
53
54
55
56
57
58
59
60
60 KO animal models showed no *Meg3* expression (**Fig. 2B**) and no detectable
61
62 *Cyp2b10* (**Fig. 2C**) activation upon chlordane treatment, consistent with the
63
64 previously reported CAR dependence of PB effects (Luisier et al. 2014). The
65
66 differential transcriptional responses observed for PB versus chlordane in humanized

CAR/PXR mice might be related to distinct, possibly species-specific, mechanisms of CAR activation by chlordane.

3.4. Proteome-based analyses of xenobiotic metabolism pathways in WT and CAR^h-PXR^h mouse liver following PB and chlordane exposure.

To further investigate the transcriptomic differences observed in CAR^h-PXR^h animals upon chlordane and PB treatments, we next performed peptide quantification using stable isotope labelling by amino acids in cell culture (SILAC) analysis of a wide range of enzymes implicated in xenobiotic metabolism using liver tissues from WT and humanized animals treated for 28 days with PB or chlordane. In WT animal samples, we found a comparable pattern of phase I cytochrome P450 protein expression following chlordane and PB treatments (**Fig. 3**). Cyp2b10, one of the strongest activated protein targets, showed significantly increased protein expression levels following both chlordane and PB treatment (**Fig. 3**). Selected proteins were strongly induced by PB but not by chlordane (e.g. Cyp2c54 and Cyp2c55), or inversely were more strongly induced by chlordane than PB (e.g. Por, Ces2a, Gstm3 and Gstm3), in WT animals (**Fig. 3, Supplementary Fig. S3 and S4**). Together these data suggest that the repertoire of xenobiotic genes activated by both compounds is largely but not fully overlapping. It is noteworthy that we also found consistent transcriptional and protein level induction in PB-treated WT mice (**Supplementary Fig. S2**). Consistent with the lower *Cyp2b10* transcriptional expression in CAR^h-PXR^h animals (**Fig 2C**), we observed reduced levels of a number of measured peptides corresponding to Cyp2b10/2b23, Cyp2c55 and Por enzymes in chlordane-treated humanized animals (**Fig.3, arrowed**). Additional Phase I and Phase II enzymes, such

1
2
3 as *Ces2a* and *Gstt3* also displayed differential activation by chlordane in the CAR^h-
4 PXR^h transgenic model (**Supplementary Fig. S3 and S4, arrowed**), suggesting that
5
6 the humanized CAR model does not conserve the ability to regulate the entire mouse
7
8 repertoire of xenobiotic metabolizing enzymes upon chlordane exposure. Together,
9
10 these results highlight potential differences in chlordane and PB modes of action.
11
12
13
14
15
16
17

18 **3.5. CAR activator specificity of *Dlk1-Dio3* lncRNA upregulation in** 19 20 **mouse liver**

21
22 We next evaluated microarray-based liver transcriptomic profiles derived from mice
23
24 treated with a panel of structurally distinct rodent non-genotoxic carcinogens that
25
26 work through distinct modes of action (studies were conducted Innovative Medicines
27
28 Initiative MARCAR consortium <http://www.imi-marcar.eu/>; original gene expression
29
30 profiling data available in Gene Expression Omnibus (GEO) under [GSE68364](#) and
31
32 [GSE60684](#)). For enhanced comparability, among all studies available, we selected
33
34 data based on (i) study duration, selecting for studies of 28 days and above duration,
35
36 at a stage when *Dlk1-Dio3* lncRNAs have been detected unambiguously upon PB
37
38 treatment in B6C3F1 or C57BL/6 mice (Lempiainen et al. 2013; Luisier et al. 2014)
39
40 and (ii) study strain, C57BL/6 studies were chosen to limit the inter-strain variability of
41
42 the response. All available compound studies fulfilling these conditions were selected
43
44 and included one cross-species CAR activator (PB), one human-specific CAR
45
46 activator (CITCO) and five rodent liver NGCs acting through alternative or
47
48 unidentified MoAs (pirinixic acid (WY), piperonyl butoxide (PBO), 1,4-dichloro-
49
50 benzene (DCB), cyproterone acetate (CPA) and methapyrilene (MPA)). Pioglitazone
51
52 (Pio), a bladder NGC in male rats, was included as a negative control compound for
53
54 mouse hepatic NGC (detailed in **Supplementary Table S1**).
55
56
57
58
59
60

1
2
3 To compare the CAR activator-dependent effects on xenobiotic metabolism, we
4
5 selected a subset of candidate CAR-dependent target genes involved in phase I and
6
7 II xenobiotic metabolism (based on published CAR^{KO}, CAR^{KO}-PXR^{KO} animal models
8
9 or on experiments conducted on PB treated hepatocytes - detailed in
10
11 **Supplementary Table S2** and references within). While we detected the expected
12
13 CAR-dependent activation of the selected xenobiotic response genes upon PB
14
15 treatment, we also observed activation of *Cyb2b10* and other selected xenobiotic
16
17 metabolism genes upon treatment with a range of distinct hepatic NGCs (**Fig. 4**).
18
19 Specifically, *Cyp2b10* expression was strongly regulated by CPA and DCB, and also
20
21 by Pioglitazone (Pio), a PPAR γ agonist that we included as a negative control for
22
23 liver NGC (Log₂FC from 6.99 to 7.67 for the three compounds, p<0.001,
24
25 **Supplementary Table S3**). These data indicate that multiple signaling pathways can
26
27 converge to mediate *Cyp* gene regulation. The CAR dependency of induction of
28
29 *Cyp2b* and *Cyp2c* gene expression upon PB treatment was confirmed in CAR^{KO}-
30
31 PXR^{KO} mice, as previously reported (Kobayashi et al. 2015).
32
33
34
35
36

37 Among the six rodent hepatic NGCs tested in this experiment, only PB treated liver
38
39 samples showed increased *Meg3* and *Rian* expression (*Meg3* Log₂FC close to 2 in
40
41 wild-type and humanized models upon 28 and 91 days of PB treatment, absent in
42
43 CAR^{KO}-PXR^{KO} animals) (**Fig. 4**). None of the other five hepatic NGCs led to a
44
45 significant induction of *Meg3* or *Rian* regardless of the mouse strains or durations of
46
47 exposure that were tested. CITCO, a direct and human-specific CAR agonist (Yang
48
49 and Wang 2014), minimally increased the expression of Phase I and Phase II genes
50
51 in CAR^h-PXR^h samples (Log₂FC= 5.94 and 2.72 in CAR^h-PXR^h mice, versus 0.69
52
53 and 0.28 in WT for *Cyp2b10* and *Cyp2c55* respectively), confirming the human
54
55 specificity of CITCO-mediated CAR activation (**Fig. 4**) (Maglich et al. 2003).
56
57
58
59
60

1
2
3 However, we did not observe significant transcriptional activation of *Meg3* and *Rian*
4
5 expression levels in humanized CAR/PXR mice under these experimental conditions.
6
7 Taken together, these results suggest that the up-regulation of *Dlk1-Dio3* lncRNA
8
9 expression represents an early biomarker for CAR activator-induced mouse liver
10
11 tumor promotion.
12
13
14
15
16
17
18
19
20
21
22
23
24
25
26
27
28
29
30
31
32
33
34
35
36
37
38
39
40
41
42
43
44
45
46
47
48
49
50
51
52
53
54
55
56
57
58
59
60

4. Discussion

Non-Genotoxic Carcinogenesis is a key safety assessment consideration for the development of chemicals and therapeutic drugs. There are currently no suitable short-term assays for predicting NGC. The identification of mechanism-based NGC biomarkers would provide industry and regulatory scientists with new tools and opportunities for earlier decision-making, mitigation of positive carcinogenicity findings and enhanced cancer risk assessment. There are, however, a number of significant challenges associated with the identification and application of NGC biomarkers (Moggs et al. 2016). Firstly, multiple combinations and chronologies of cancer hallmarks contribute to tumorigenicity and thus the detection of individual drug-induced neoplastic risk molecular indicators is not likely to be optimal for predicting diverse mechanisms of xenobiotic-induced carcinogenesis. Secondly, the identification of predictive transcriptomic NGC biomarkers in rodent carcinogenicity studies is confounded by the heterogeneity of drug-induced rodent tumors that cover a broad range of tissue-, gender-, strain- and species-specific mechanisms. Furthermore, the potential contributions from on- or off-target properties of NGC compounds makes the determination of mode of action and assessment of human relevance very challenging.

Nevertheless, mechanistic studies that integrate phenotypically-anchored molecular and biochemical biomarkers can be used to support the interpretation of drug-induced tumors and in some cases provide valuable perspectives on potential relevance in humans. Although numerous publications report extensive efforts to identify predictive transcriptomic biomarkers for NGC, this has proved challenging even for a single target organ such as the liver (Kossler et al. 2015; Ellinger-Ziegelbauer et al. 2011; Fielden et al. 2011). We propose that the validation of such

1
2
3 molecular biomarkers will be greatly enhanced by establishing functional
4 relationships to known cancer hallmarks. This is exemplified by the identification of
5 *Dlk1-Dio3* imprinted gene cluster non-coding RNAs as novel candidate biomarkers
6 for phenobarbital-induced liver tumor promotion (Lempiainen et al. 2013). The
7 induction of *Dlk1-Dio3* non-coding RNAs by phenobarbital is dependent on both
8 constitutive androstane receptor (CAR) and β -catenin signalling pathways, consistent
9 with a CAR activator-mediated hepatocarcinogenesis mode of action. Importantly,
10 *Dlk1-Dio3* non-coding RNAs have recently been associated with stem cell
11 pluripotency in mice and various neoplasms in humans. In addition, the perivenous
12 localization of phenobarbital-induced *Dlk1-Dio3* non-coding RNAs occurs in a region
13 of the liver that was recently associated with Wnt signalling-dependent stem cell-like
14 properties (Wang et al. 2015; Planas-Paz et al. 2016). Together, these functional
15 relationships imply that sub-population of hepatocytes may be prone to drug-induced
16 reprogramming and de-differentiation and that biomarkers such as *Dlk1-Dio3* non-
17 coding RNAs might serve as useful early molecular indicators for CAR-mediated
18 hepatocarcinogenesis (**Supplementary Figure S5**).

19
20
21 Specifically, in this paper, we have compared phenotypic, histopathological,
22 transcriptional and proteomic responses following treatment with the cross-species
23 CAR activators, PB and chlordane, and further compared key transcriptional
24 signatures with seven other NGC compounds working through a range of MoAs
25 (**Supplementary Table S1**), including the human-specific direct CAR activator
26 CITCO. We find that the xenobiotic metabolism gene *Cyp2b10* is upregulated by
27 several distinct hepatic NGCs as well as the PPAR γ agonist Pioglitazone (a control
28 comparator compound that is not associated with hepatic NGC). Although *Cyp2b10*
29 induction in drug-induced mouse liver tumors has previously been proposed as a
30
31
32
33
34
35
36
37
38
39
40
41
42
43
44
45
46
47
48
49
50
51
52
53
54
55
56
57
58
59
60

1
2
3 surrogate biomarker of CAR activation (Hoflack et al. 2012), our data suggest that
4
5 Cyp2b10 induction alone may lack the required specificity for an early mechanism-
6
7 based biomarker of CAR-mediated NGC consistent with previous observations that
8
9 induction of CYP2B1/2 liver enzymes failed to correlate with rodent NGC (Elcombe et
10
11 al. 2002). In contrast, our data provide additional support to the CAR activator
12
13 specificity of previously identified *Dlk1-Dio3* lncRNA candidate biomarkers for mouse
14
15 liver tumor promotion (Lempiainen et al. 2013).
16
17

18
19 Since we used double transgenic (CAR^{KO} - PXR^{KO} and CAR^h - PXR^h) animals in the PB
20
21 and chlordane *in vivo* studies, we cannot formally exclude the role of PXR activation
22
23 and function in the identified molecular signature. CAR shares several common
24
25 features with PXR, and they overlap at a number of target genes and xenobiotic
26
27 activators (Yang and Wang 2014). Although previous studies in CAR and PXR KO
28
29 models also identified differentially regulated xenobiotic targets (Maglich et al. 2002;
30
31 Wei et al. 2002; Cui and Klaassen 2016), the strict specificity to CAR versus PXR
32
33 may require further investigations.
34
35
36

37
38 While both cross-species CAR activators, PB and chlordane, led to *Dlk1-Dio3*
39
40 lncRNA activation, consistent with its direct human CAR activation MoA (Maglich et
41
42 al. 2003), CITCO did not lead to either xenobiotic genes or *Dlk1-Dio3* cluster lncRNA
43
44 activation in WT animals (**Fig. 4**) and led to moderate *Cyp2b10* activation, without
45
46 effect on *Dlk1-Dio3* lncRNAs in CAR/PXR humanized animals. The absence of
47
48 lncRNA activation by CITCO is reminiscent of the significantly decreased lncRNA
49
50 activation upon chlordane exposure in humanized animals and could be related to
51
52 species-specific interactions upstream or downstream of CAR/PXR activation that
53
54 could be perturbed in the human transgenic model (**Fig. 5**). In addition, CITCO acts
55
56 through direct CAR binding and activation, and a conformational change of the hCAR
57
58
59

1
2
3 isoforms in transgenic animals might also explain the apparent differences in Cyp
4 induction and lack of *Dlk1-Dio3* cluster activation. Alternatively, the exposure or
5 duration of the study in the transgenic animal studies may not be sufficient to detect
6
7
8
9
10 *Dlk1-Dio3* lncRNA activation. Finally, we note that only two long non-coding RNAs
11 (*Meg3* and *Rian*) are represented on the microarray used to profile compounds in
12
13 **Fig. 4** and thus we cannot exclude that CITCO induces alternate *Dlk1-Dio3* ncRNAs.
14
15 Further analyses of the complete *Dlk1-Dio3* cluster transcriptional landscape
16 following longer-term CITCO treatment in PXR^h-CAR^h animals would be necessary to
17 extend these observations as well as to explore the relevance of this compound in
18 liver carcinogenesis. Three of the compounds tested (CPA, DCB and Pio), in addition
19 to PB and CITCO, led to significant activation of *Cyp2b10* and *Cyp2c55*. However,
20 under the experimental conditions tested, they did not induce detectable microarray-
21 based dysregulation of *Dlk1-Dio3* cluster lncRNAs *Meg3* or *Rian*. Interestingly, using
22 CYP2B6LacZ reporter and CAR/PXR humanized mouse models, both DCB and CPA
23 were recently characterized as CAR activators with DCB displaying a higher potency
24 towards human CAR than mouse CAR, and CPA activating both CAR and PXR
25 (CJH, CRW, unpublished, manuscript in preparation). While no microarray-based
26 upregulation of the *Dlk1-Dio3* lncRNAs *Meg3* and *Rian* was detected for either DCB
27 or CPA, quantitative PCR-based expression data indicated upregulation of several
28 non-coding miRNAs within the *Dlk1-Dio3* cluster for both of these compounds
29 (unpublished MARCAR data), consistent with our proposal that CAR-activation leads
30 to *Dlk1-Dio3* cluster ncRNA perturbations in liver NGC models. It is noteworthy that
31 the *Dlk1-Dio3* cluster encodes one of the largest microRNA clusters in the
32 mammalian genome, as well as numerous small nucleolar RNAs (snoRNAs). We
33 previously demonstrated PB-mediated induction both lncRNAs and miRNAs from the
34 *Dlk1-Dio3* locus (Lempiainen et al. 2013). Interestingly, some *Dlk1-Dio3* cluster
35
36
37
38
39
40
41
42
43
44
45
46
47
48
49
50
51
52
53
54
55
56
57
58
59
60

1
2
3 miRNAs appear to be transcribed as single polycistronic unit (Fiore et al. 2009) and
4
5 many of these miRNAs have been reported to be differentially expressed in
6
7 pathologic processes including various cancers (reviewed in (Benetatos et al. 2013)).
8
9 In this manuscript we have evaluated the hepatic responsiveness of four *Dlk1-Dio3*
10
11 cluster long-non-coding RNAs (Meg3, anti-Rtl1, Rian, Mirg) by qPCR (PB and
12
13 chlordanane), and of two *Dlk1-Dio3* cluster long-non-coding RNA (Meg3 and Rian) by
14
15 microarray-based transcript profiling (panel of compounds in **Fig. 4**). We cannot
16
17 exclude that the compounds tested induce further broad or specific changes of the
18
19 *Dlk1-Dio3* non-coding RNAs landscape and thus further RNA-sequencing based
20
21 assessments of *Dlk1-Dio3* ncRNA candidate biomarkers is warranted. Beyond their
22
23 association with pluripotency (Liu et al. 2010; Stadtfeld and Hochedlinger 2010), the
24
25 interest in investigating the expression profile on the *Dlk1-Dio3* cluster lncRNAs, has
26
27 been reinforced by the discovery that they are able to form complexes with the
28
29 epigenetic machinery, including Polycomb group proteins (Kaneko et al. 2014) and
30
31 might be targeted to specific genes through the formation of RNA-DNA triplex
32
33 structures (Mondal et al. 2015). These regulatory interactions (illustrated
34
35
36
37
38 **Supplementary Figure S5**) could play an important role in cellular transformation.
39
40
41
42
43
44
45
46
47
48
49
50
51
52
53
54
55
56
57
58
59
60

5. Conclusions

In the present study we have demonstrated that a second CAR activator and mouse liver non-genotoxic carcinogen (i.e. chlordane) robustly induces perivenous *Dlk1-Dio3* non-coding RNA expression and we provide preliminary evidence that this candidate biomarker signature may indeed be specific for CAR-mediated hepatocarcinogenesis. Through comparing the response to chlordane and PB exposure in WT and humanized animals, we also point to the existence of undetermined co-effector phenomenon, upstream or downstream to CAR activation (**Fig. 5**). Since significant molecular, cellular and pathophysiologic differences exist between mammalian species and strains, further evaluation of *Dlk1-Dio3* cluster non-coding RNA functions, biomarker detection sensitivity, MoA specificity and human relevance, is warranted prior to use as an early indicator for CAR-mediated hepatocarcinogenesis. In particular, mapping species differences in the hepatic chromatin architecture of candidate non-genotoxic carcinogen effector genes such as *Dlk1-Dio3* ncRNAs may help predict the potential for NGC-mediated modulation in humans (AV, RT and JM, unpublished data).

Acknowledgements, Funding and conflicts of interest

Innovative Medicine Initiative Joint Undertaking (IMI JU) (115001) (MARCAR project; <http://www.imi-marcar.eu/>). This work was also supported by Cancer Research UK program grant C4639/A10822 awarded to C.R.W. All IMI-MARCAR consortium partners had a role in study design, data collection and analysis, decision to publish, or preparation of the manuscript. We would like to thank Sarah Brasa, Harri Lempiäinen for experimental and *in vivo* study support and Serge Winter and Wei Wu for the pharmacokinetics analyses of chlordane and Phenobarbital studies. We would like also to thank Chi-Hse Teng for the statistical analysis support. M.G., M.W., V.D., D.P.S., B.D., P.M., J.G.M. and R.T. are full time employees of Novartis Pharma. A.V. is a recipient of a Novartis Institutes for Biomedical Research Postdoctoral Fellowships. H.E.Z. is a full time employee of Bayer. C.R.E. is a full time employee of CXR Biosciences.

References

- Aydinlik, H., T. D. Nguyen, O. Moennikes, A. Buchmann, and M. Schwarz. 2001. 'Selective pressure during tumor promotion by phenobarbital leads to clonal outgrowth of beta-catenin-mutated mouse liver tumors', *Oncogene*, 20: 7812-6.
- Barrass, N., M. Stewart, S. Warburton, J. Aitchison, D. Jackson, P. Wadsworth, A. Marsden, and T. Orton. 1993. 'Cell proliferation in the liver and thyroid of C57Bl/10J mice after dietary administration of chlordane', *Environ Health Perspect*, 101 Suppl 5: 219-23.
- Benetatos, L., E. Hatzimichael, E. Londin, G. Vartholomatos, P. Loher, I. Rigoutsos, and E. Briasoulis. 2013. 'The microRNAs within the DLK1-DIO3 genomic region: involvement in disease pathogenesis', *Cell Mol Life Sci*, 70: 795-814.
- Benetatos, L., G. Vartholomatos, and E. Hatzimichael. 2014. 'DLK1-DIO3 imprinted cluster in induced pluripotency: landscape in the mist', *Cell Mol Life Sci*, 71: 4421-30.
- Braeuning, A., R. Sanna, J. Huelsken, and M. Schwarz. 2009. 'Inducibility of drug-metabolizing enzymes by xenobiotics in mice with liver-specific knockout of *Cttnb1*', *Drug Metab Dispos*, 37: 1138-45.
- Cox, J., and M. Mann. 2008. 'MaxQuant enables high peptide identification rates, individualized p.p.b.-range mass accuracies and proteome-wide protein quantification', *Nat Biotechnol*, 26: 1367-72.
- Cui, J. Y., and C. D. Klaassen. 2016. 'RNA-Seq reveals common and unique PXR- and CAR-target gene signatures in the mouse liver transcriptome', *Biochim Biophys Acta*.
- Cui, W., Z. Huang, H. He, N. Gu, G. Qin, J. Lv, T. Zheng, K. Sugimoto, and Q. Wu. 2015. 'MiR-1188 at the imprinted *Dlk1-Dio3* domain acts as a tumor suppressor in hepatoma cells', *Mol Biol Cell*, 26: 1416-27.
- Elcombe, C. R., J. Odum, J. R. Foster, S. Stone, S. Haslam, A. R. Soames, I. Kimber, and J. Ashby. 2002. 'Prediction of rodent nongenotoxic carcinogenesis: evaluation of biochemical and tissue changes in rodents following exposure to nine nongenotoxic NTP carcinogens', *Environ Health Perspect*, 110: 363-75.
- Ellinger-Ziegelbauer, H., M. Adler, A. Amberg, A. Brandenburg, J. J. Callanan, S. Connor, M. Fountoulakis, H. Gmuender, A. Gruhler, P. Hewitt, M. Hodson, K. A. Matheis, D. McCarthy, M. Raschke, B. Riefke, C. S. Schmitt, M. Sieber, A. Sposny, L. Suter, B. Sweatman, and A. Mally. 2011. 'The enhanced value of combining conventional and "omics" analyses in early assessment of drug-induced hepatobiliary injury', *Toxicol Appl Pharmacol*, 252: 97-111.
- Fielden, M. R., A. Adai, R. T. Dunn, 2nd, A. Olaharski, G. Searfoss, J. Sina, J. Aubrecht, E. Boitier, P. Nioi, S. Auerbach, D. Jacobson-Kram, N. Raghavan, Y. Yang, A. Kincaid, J. Sherlock, S. J. Chen, B. Car, and Carcinogenicity Working Group Predictive Safety Testing Consortium. 2011. 'Development and evaluation of a genomic signature for the prediction and mechanistic assessment of nongenotoxic hepatocarcinogens in the rat', *Toxicol Sci*, 124: 54-74.
- Fiore, R., S. Khudayberdiev, M. Christensen, G. Siegel, S. W. Flavell, T. K. Kim, M. E. Greenberg, and G. Schrott. 2009. 'Mef2-mediated transcription of the

- miR379-410 cluster regulates activity-dependent dendritogenesis by fine-tuning Pumilio2 protein levels', *EMBO J*, 28: 697-710.
- Hoflack, J. C., L. Mueller, S. Fowler, A. Braendli-Baiocco, N. Flint, O. Kuhlmann, T. Singer, and A. Roth. 2012. 'Monitoring Cyp2b10 mRNA expression at cessation of 2-year carcinogenesis bioassay in mouse liver provides evidence for a carcinogenic mechanism devoid of human relevance: the dalcetrapib experience', *Toxicol Appl Pharmacol*, 259: 355-65.
- Huang, W., J. Zhang, M. Washington, J. Liu, J. M. Parant, G. Lozano, and D. D. Moore. 2005. 'Xenobiotic stress induces hepatomegaly and liver tumors via the nuclear receptor constitutive androstane receptor', *Mol Endocrinol*, 19: 1646-53.
- Kaneko, S., R. Bonasio, R. Saldana-Meyer, T. Yoshida, J. Son, K. Nishino, A. Umezawa, and D. Reinberg. 2014. 'Interactions between JARID2 and noncoding RNAs regulate PRC2 recruitment to chromatin', *Mol Cell*, 53: 290-300.
- Klipper-Aurbach, Y., M. Wasserman, N. Braunspiegel-Weintrob, D. Borstein, S. Peleg, S. Assa, M. Karp, Y. Benjamini, Y. Hochberg, and Z. Laron. 1995. 'Mathematical formulae for the prediction of the residual beta cell function during the first two years of disease in children and adolescents with insulin-dependent diabetes mellitus', *Med Hypotheses*, 45: 486-90.
- Kobayashi, K., M. Hashimoto, P. Honkakoski, and M. Negishi. 2015. 'Regulation of gene expression by CAR: an update', *Arch Toxicol*, 89: 1045-55.
- Kossler, N., K. A. Matheis, N. Ostenfeldt, D. Bach Toft, S. Dhalluin, U. Deschl, and A. Kalkuhl. 2015. 'Identification of specific mRNA signatures as fingerprints for carcinogenesis in mice induced by genotoxic and nongenotoxic hepatocarcinogens', *Toxicol Sci*, 143: 277-95.
- Lempiainen, H., P. Couttet, F. Bolognani, A. Muller, V. Dubost, R. Luisier, A. Del Rio Espinola, V. Vitry, E. B. Unterberger, J. P. Thomson, F. Treindl, U. Metzger, C. Wrzodek, F. Hahne, T. Zollinger, S. Brasa, M. Kalteis, M. Marcellin, F. Giudicelli, A. Braeuning, L. Morawiec, N. Zamurovic, U. Langle, N. Scheer, D. Schubeler, J. Goodman, S. D. Chibout, J. Marlowe, D. Theil, D. J. Heard, O. Grenet, A. Zell, M. F. Templin, R. R. Meehan, R. C. Wolf, C. R. Elcombe, M. Schwarz, P. Moulin, R. Terranova, and J. G. Moggs. 2013. 'Identification of Dlk1-Dio3 imprinted gene cluster noncoding RNAs as novel candidate biomarkers for liver tumor promotion', *Toxicol Sci*, 131: 375-86.
- Liu, L., G. Z. Luo, W. Yang, X. Zhao, Q. Zheng, Z. Lv, W. Li, H. J. Wu, L. Wang, X. J. Wang, and Q. Zhou. 2010. 'Activation of the imprinted Dlk1-Dio3 region correlates with pluripotency levels of mouse stem cells', *J Biol Chem*, 285: 19483-90.
- Loeppen, S., D. Schneider, F. Gaunitz, R. Gebhardt, R. Kurek, A. Buchmann, and M. Schwarz. 2002. 'Overexpression of glutamine synthetase is associated with beta-catenin-mutations in mouse liver tumors during promotion of hepatocarcinogenesis by phenobarbital', *Cancer Res*, 62: 5685-8.
- Luisier, R., H. Lempiainen, N. Scherbichler, A. Braeuning, M. Geissler, V. Dubost, A. Muller, N. Scheer, S. D. Chibout, H. Hara, F. Picard, D. Theil, P. Couttet, A. Vitobello, O. Grenet, B. Grasl-Kraupp, H. Ellinger-Ziegelbauer, J. P. Thomson, R. R. Meehan, C. R. Elcombe, C. J. Henderson, C. R. Wolf, M. Schwarz, P. Moulin, R. Terranova, and J. G. Moggs. 2014. 'Phenobarbital induces cell cycle transcriptional responses in mouse liver humanized for constitutive androstane and pregnane x receptors', *Toxicol Sci*, 139: 501-11.

- 1
2
3 Luk, J. M., J. Burchard, C. Zhang, A. M. Liu, K. F. Wong, F. H. Shek, N. P. Lee, S. T.
4 Fan, R. T. Poon, I. Ivanovska, U. Philippar, M. A. Cleary, C. A. Buser, P. M.
5 Shaw, C. N. Lee, D. G. Tenen, H. Dai, and M. Mao. 2011. 'DLK1-DIO3
6 genomic imprinted microRNA cluster at 14q32.2 defines a stemlike subtype of
7 hepatocellular carcinoma associated with poor survival', *J Biol Chem*, 286:
8 30706-13.
- 9
10 MacLeod, A. K., P. G. Fallon, S. Sharp, C. J. Henderson, C. R. Wolf, and J. T.
11 Huang. 2015. 'An enhanced in vivo stable isotope labeling by amino acids in
12 cell culture (SILAC) model for quantification of drug metabolism enzymes', *Mol*
13 *Cell Proteomics*, 14: 750-60.
- 14 Maglich, J. M., D. J. Parks, L. B. Moore, J. L. Collins, B. Goodwin, A. N. Billin, C. A.
15 Stoltz, S. A. Kliewer, M. H. Lambert, T. M. Willson, and J. T. Moore. 2003.
16 'Identification of a novel human constitutive androstane receptor (CAR)
17 agonist and its use in the identification of CAR target genes', *J Biol Chem*,
18 278: 17277-83.
- 19
20 Maglich, J. M., C. M. Stoltz, B. Goodwin, D. Hawkins-Brown, J. T. Moore, and S. A.
21 Kliewer. 2002. 'Nuclear pregnane x receptor and constitutive androstane
22 receptor regulate overlapping but distinct sets of genes involved in xenobiotic
23 detoxification', *Mol Pharmacol*, 62: 638-46.
- 24 Malarkey, David E. 1995. '<Carcinogenesis-1995-Malarkey-Chlordane.pdf>',
25 *Carcinogenesis*, 16: 2617-25.
- 26 Moggs, Jonathan G., Timothy MacLachlan, Hans-Joerg Martus, and Philip Bentley.
27 2016. 'Derisking Drug-Induced Carcinogenicity for Novel Therapeutics', *Trends*
28 *in Cancer*, 2: 398-408.
- 29
30 Mondal, T., S. Subhash, R. Vaid, S. Enroth, S. Uday, B. Reinius, S. Mitra, A.
31 Mohammed, A. R. James, E. Hoberg, A. Moustakas, U. Gyllenstein, S. J.
32 Jones, C. M. Gustafsson, A. H. Sims, F. Westerlund, E. Gorab, and C.
33 Kanduri. 2015. 'MEG3 long noncoding RNA regulates the TGF-beta pathway
34 genes through formation of RNA-DNA triplex structures', *Nat Commun*, 6:
35 7743.
- 36 Moser, G. J., and R. C. Smart. 1989. 'Hepatic tumor-promoting chlorinated
37 hydrocarbons stimulate protein kinase C activity', *Carcinogenesis*, 10: 851-6.
- 38 Mutoh, S., M. Sobhany, R. Moore, L. Perera, L. Pedersen, T. Sueyoshi, and M.
39 Negishi. 2013. 'Phenobarbital indirectly activates the constitutive active
40 androstane receptor (CAR) by inhibition of epidermal growth factor receptor
41 signaling', *Sci Signal*, 6: ra31.
- 42
43 Omura, K., T. Uehara, Y. Morikawa, H. Hayashi, K. Mitsumori, K. Minami, M. Kanki,
44 H. Yamada, A. Ono, and T. Urushidani. 2014. 'Detection of initiating potential
45 of non-genotoxic carcinogens in a two-stage hepatocarcinogenesis study in
46 rats', *J Toxicol Sci*, 39: 785-94.
- 47 Planas-Paz, L., V. Orsini, L. Boulter, D. Calabrese, M. Pikiólek, F. Nigsch, Y. Xie, G.
48 Roma, A. Donovan, P. Marti, N. Beckmann, M. T. Dill, W. Carbone, S.
49 Bergling, A. Isken, M. Mueller, B. Kinzel, Y. Yang, X. Mao, T. B. Nicholson, R.
50 Zamponi, P. Capodiceci, R. Valdez, D. Rivera, A. Loew, C. Ukomadu, L. M.
51 Terracciano, T. Bouwmeester, F. Cong, M. H. Heim, S. J. Forbes, H. Ruffner,
52 and J. S. Tchorz. 2016. 'The RSPO-LGR4/5-ZNRF3/RNF43 module controls
53 liver zonation and size', *Nat Cell Biol*, 18: 467-79.
- 54
55 Rignall, B., A. Braeuning, A. Buchmann, and M. Schwarz. 2011. 'Tumor formation in
56 liver of conditional beta-catenin-deficient mice exposed to a
57 diethylnitrosamine/phenobarbital tumor promotion regimen', *Carcinogenesis*,
58 32: 52-7.

- 1
2
3 Ross, J., S. M. Plummer, A. Rode, N. Scheer, C. C. Bower, O. Vogel, C. J.
4 Henderson, C. R. Wolf, and C. R. Elcombe. 2010. 'Human constitutive
5 androstane receptor (CAR) and pregnane X receptor (PXR) support the
6 hypertrophic but not the hyperplastic response to the murine nongenotoxic
7 hepatocarcinogens phenobarbital and chlordane in vivo', *Toxicol Sci*, 116:
8 452-66.
- 9
10 Ruch, R. J., R. Fransson, S. Flodstrom, L. Warngard, and J. E. Klaunig. 1990.
11 'Inhibition of hepatocyte gap junctional intercellular communication by
12 endosulfan, chlordane and heptachlor', *Carcinogenesis*, 11: 1097-101.
- 13 Smyth, G. K., J. Michaud, and H. S. Scott. 2005. 'Use of within-array replicate spots
14 for assessing differential expression in microarray experiments',
15 *Bioinformatics*, 21: 2067-75.
- 16 Stadtfeld, M., and K. Hochedlinger. 2010. 'Induced pluripotency: history,
17 mechanisms, and applications', *Genes Dev*, 24: 2239-63.
- 18 Unterberger, E. B., J. Eichner, C. Wrzodek, H. Lempiainen, R. Luisier, R. Terranova,
19 U. Metzger, S. Plummer, T. Knorpp, A. Braeuning, J. Moggs, M. F. Templin, V.
20 Honndorf, M. Piotto, A. Zell, and M. Schwarz. 2014. 'Ha-ras and beta-catenin
21 oncoproteins orchestrate metabolic programs in mouse liver tumors', *Int J*
22 *Cancer*, 135: 1574-85.
- 23
24 Wang, B., L. Zhao, M. Fish, C. Y. Logan, and R. Nusse. 2015. 'Self-renewing diploid
25 Axin2(+) cells fuel homeostatic renewal of the liver', *Nature*, 524: 180-5.
- 26 Wei, P., J. Zhang, D. H. Dowhan, Y. Han, and D. D. Moore. 2002. 'Specific and
27 overlapping functions of the nuclear hormone receptors CAR and PXR in
28 xenobiotic response', *Pharmacogenomics J*, 2: 117-26.
- 29
30 Whysner, J., F. Montandon, R. M. McClain, J. Downing, L. K. Verna, R. E. Steward,
31 3rd, and G. M. Williams. 1998. 'Absence of DNA adduct formation by
32 phenobarbital, polychlorinated biphenyls, and chlordane in mouse liver using
33 the 32P-postlabeling assay', *Toxicol Appl Pharmacol*, 148: 14-23.
- 34 Xu, W. P., M. Yi, Q. Q. Li, W. P. Zhou, W. M. Cong, Y. Yang, B. F. Ning, C. Yin, Z. W.
35 Huang, J. Wang, H. Qian, C. F. Jiang, Y. X. Chen, C. Y. Xia, H. Y. Wang, X.
36 Zhang, and W. F. Xie. 2013. 'Perturbation of MicroRNA-370/Lin-28 homolog
37 A/nuclear factor kappa B regulatory circuit contributes to the development of
38 hepatocellular carcinoma', *Hepatology*, 58: 1977-91.
- 39
40 Yamamoto, Y., R. Moore, T. L. Goldsworthy, M. Negishi, and R. R. Maronpot. 2004.
41 'The orphan nuclear receptor constitutive active/androstane receptor is
42 essential for liver tumor promotion by phenobarbital in mice', *Cancer Res*, 64:
43 7197-200.
- 44 Yang, H., and H. Wang. 2014. 'Signaling control of the constitutive androstane
45 receptor (CAR)', *Protein Cell*, 5: 113-23.
- 46 Yin, C., P. Q. Wang, W. P. Xu, Y. Yang, Q. Zhang, B. F. Ning, P. P. Zhang, W. P.
47 Zhou, W. F. Xie, W. S. Chen, and X. Zhang. 2013. 'Hepatocyte nuclear factor-
48 4alpha reverses malignancy of hepatocellular carcinoma through regulating
49 miR-134 in the DLK1-DIO3 region', *Hepatology*, 58: 1964-76.
- 50
51 Zucker, E. . 1985. "Hazard Evaluation Division Standard Evaluation Procedure: Acute
52 Toxicity Test for
53
54 Freshwater Fish." In, edited by National Technical U.S. Environmental Protection
55 Agency and VA Information Service: Springfield.
- 56
57
58
59
60

Figure Legends

Figure 1. *Dlk1-Dio3* cluster response upon 28 days phenobarbital or chlordane exposure. (A) Experimental design of the chlordane and PB studies for molecular and phenotypic profiling (B) Architecture of *Dlk1-Dio3* genomic region illustrating parent-of-origin transcripts and differentially methylated regions (DMR) – methylated regions are represented with solid circles. (C) RT-qPCR analysis of *Dlk1-Dio3* genes (*Dlk1* and *Dio3*) and long non-coding RNAs (*Meg3*, *anti-Rtl1*, *Rian*, *Mirg*) expression in wild type (WT) mouse livers treated for 28 days with PB, chlordane or the relevant vehicle controls. Expression levels are indicated as mean \pm SEM (n=5 biological replicates/group). Data were analyzed using GraphPad Prism 7.0. Statistical significance of treated versus untreated (vehicle) qPCR signal differences were tested using unpaired t-tests with Welch's correction for unequal variance, *p<0.05, **p<0.01. (D) *Meg3* *in situ* hybridization and GS immunohistochemistry in 28 days PB or in chlordane treated livers with indicated vehicle controls. Water (H₂O), Corn Oil (CO).

Figure 2. *Dlk1-Dio3* cluster lncRNAs are differentially induced by PB and chlordane in humanized CAR/PXR animals. (A) *Dlk1-Dio3* coding and non-coding RNAs expression analysis in CAR^h-PXR^h mice after 28 days chlordane or PB exposure (t=28d), in comparison to indicated vehicle control treatments. (B) *Meg3* expression analysis in WT and CAR^{KO}/PXR^{KO} mice after 28 days of chlordane treatment (t=28d) as compared to vehicle treated samples. (C) *Cyp2b10* expression analyses across indicated mouse models after 28 days PB or chlordane treatment (t=28d). (D) human *CAR* (*hCAR*) expression analysis across indicated mouse models after 28 days of treatments (t=28d). Expression levels are indicated as mean \pm SEM (n=5 biological replicates/group). Data were analyzed using GraphPad Prism 7.0. All

1
2
3 expression analyses are based on qPCR, primer sequences are provided in
4
5 (Lempiainen et al. 2013) and Supplementary Materials and Methods. Statistical
6
7 significance of treated versus untreated (vehicle) qPCR signal differences were
8
9 tested using unpaired t-tests with Welch's correction for unequal variance, * $p < 0.05$,
10
11 ** $p < 0.01$, *** $p < 0.001$, **** $p < 0.0001$. Vehicle controls: Water (H₂O) and Corn Oil
12
13 (CO).
14
15
16
17
18
19

20 **Figure 3. Proteomic analysis of Phase I cytochrome P450 (Cyp) expression in**
21 **WT and CAR^h PXR^h mice.** Quantitative measurement of peptides using *in vivo*
22 'stable isotope labeling with amino acids in cell culture' (SILAC) technique from PB
23 treated (A) and chlordane treated (B) liver samples, in comparison with indicated
24 vehicle controls, in WT (filled bars) and in CAR^h/PXR^h (hatched bars) mice after 28
25 days of treatment (t=28d). Corresponding proteins are named on the X axis; the Y
26 axis is expressed in fold change expression, based of vehicle expression value.
27
28 Arrows indicate the metabolic enzymes concerned by the decreased signal in
29 chlordane treated CAR^h/PXR^h samples as compared to WT samples. Protein levels
30 are indicated as mean \pm SEM (H₂O and phenobarbital n=5 biological
31 replicates/group; CO and Chlordane n=3 biological replicates/group). Data were
32 analyzed using GraphPad Prism 7.0. Statistical significance of treated versus
33 untreated (vehicle) signal differences were tested using multiple unpaired t-tests on
34 log₂ transformed data. The p-values were adjusted using Holm-Sidak method,
35
36 * $p < 0.05$, ** $p < 0.01$, *** $p < 0.001$. Vehicle controls: Water (H₂O) and Corn Oil (CO)
37
38
39
40
41
42
43
44
45
46
47
48
49
50
51
52
53
54
55
56
57
58
59
60

1
2
3 **Figure 4. Cross-compound comparison of microarray-based xenobiotic**
4 **metabolism and *Dlk1-Dio3* lncRNAs transcriptional expression profiles.** *In vivo*
5 study samples from indicated compound classes were profiled by Affymetrix
6 microarray and specific gene expression signatures (phase I and phase II xenobiotic
7 genes and progressive *Dlk1-Dio3* encoded Meg3 lncRNA expression) extracted and
8 compared. Probes set expression values were summarized by gene and expressed
9 in Log₂ fold change (Log₂FC) expression, calculated on the average of the 5
10 replicates (treated *versus* control). Significant difference between vehicle and treated
11 conditions were tested with the limma package with the Benjamini-Hochberg method
12 correction applied (Klipper-Aurbach et al. 1995; Smyth, Michaud, and Scott 2005),
13 *p<0.05, **p<0.01, ***p<0.001, ****p<0.0001. NGC: Non-genotoxic carcinogen, NC:
14 non-carcinogen, CPA: cyproterone acetate, DCB: 1,4-dichlorobenzene, Mpy:
15 Methapyrilene, PB: phenobarbital, PBO: piperonyl butoxide, Wy: pirinixic acid, Pio:
16 pioglitazone.
17
18
19
20
21
22
23
24
25
26
27
28
29
30
31
32
33
34
35
36
37

38 **Figure 5. Updated model for NGC-induced perturbation of the *Dlk1-Dio3* cluster**
39 **lncRNA and xenobiotic response** (modified from (Lempiainen et al. 2013)). Direct
40 CAR activators or indirect compounds acting through cellular transducers (green
41 triangle, e.g. as described in (Mutoh et al. 2013)) regulate the expression of CAR-
42 dependent xenobiotic genes. The β -catenin pathway regulates expression of
43 xenobiotic metabolic genes in a context dependent manner (Braeuning et al. 2009).
44 Within WNT positive domains (e.g. perivenous hepatocytes) CAR activation is also
45 associated with *Dlk1-Dio3* cluster ncRNAs expression. The current model
46 acknowledges the presence of intermediate/uncharacterized co-effectors (orange
47 hexagons) acting downstream CAR activation, and possibly linking the constitutive
48
49
50
51
52
53
54
55
56
57
58
59
60 33

1
2
3 xenobiotic metabolism and the progressive CAR/ β -catenin dependent response. The
4
5 upregulation of *Dlk1-Dio3* cluster ncRNAs might contribute to hepatocyte hypertrophy
6
7 and reprogramming (Luk et al. 2011), while xenobiotic response may lead to
8
9 oxidative stress through the production of reactive metabolites (Omura et al. 2014),
10
11 both contributing potential key events in drug-induced tumor promotion.
12
13
14
15
16
17
18
19
20
21
22
23
24
25
26
27
28
29
30
31
32
33
34
35
36
37
38
39
40
41
42
43
44
45
46
47
48
49
50
51
52
53
54
55
56
57
58
59
60

Supplementary Figure legends

Supplementary Figure S1. RT-qPCR analyses of *Dlk1-Dio3* cluster and *Cyp2b10* gene expression following 28 day compound withdrawal. Gene expression measurement of (A) *Dlk1-Dio3* coding (*Dlk1* and *Dio3*) and non-coding RNAs (*Meg3*, *anti-Rtl1*, *Rian*, *Mirg*) and (B) *Cyp2b10* after treatment regimen (t=91 days in H₂O-phenobarbital study and t=28 days in CO-chlordane study) followed by 28 days of compound withdrawal (t=119 and t=56 days respectively). Expression levels are indicated as mean \pm SEM (n=5 biological replicates/group). Data were analyzed using GraphPad Prism 7.0. Statistical significance of treated versus untreated (vehicle) qPCR signal differences were tested using unpaired t-tests with Welch's correction for unequal variance, *p<0.05, **p<0.01, ***p<0.001. Vehicle controls: Water (H₂O) and Corn Oil (CO).

Supplementary Figure S2. Proteomics and gene expression profiles comparison of a panel of PB-responsive xenobiotic metabolism proteins. Probes set expression values were summarized by (A) gene, and (B) protein expression, deducted from SILAC peptide measurement, are expressed in log₂ fold change (Log₂FC) expression, calculated on the average of the 5 replicates (treated *versus* control). Vh_1016 to Vh_1020 and WT_V1 to WT_V5 correspond to vehicle treated samples, PB_2016 to PB_2020 and WT_PB1 to WT_PB5 correspond to Phenobarbital treated samples for gene expression and protein expression analyses respectively. Hierarchical clustering was performed for individual animal group and gene/protein expression.

1
2
3 **Supplementary Figure S3. Proteomics analysis of non-Cyp phase I protein**
4 **expression in WT and CAR^h PXR^h mice.** Quantitative measurement of peptides
5 using the 'stable isotope labeling with amino acids in cell culture' (SILAC) technique
6 from (A) PB treated and (B) chlordane treated liver samples, in WT (filled bars) and in
7 CAR^h PXR^h (hatched bars) mice. Corresponding proteins are named on the X axis;
8 the Y axis is expressed in fold change expression, based of vehicle expression value.
9
10 Arrows indicate the metabolic enzymes concerned by the decreased signal in
11 chlordane treated CAR^h/PXR^h samples as compared to WT samples. Protein levels
12 are indicated as mean ± SEM (H₂O and phenobarbital n=5 biological
13 replicates/group; CO and Chlordane n=3 biological replicates/group).Data were
14 analyzed using GraphPad Prism 7.0. Statistical significance of treated versus
15 untreated (vehicle) signal differences were tested using multiple unpaired t-tests on
16 log₂ transformed data. The p-values were adjusted using Holm-Sidak method,
17 *p<0.05, **p<0.01. Vehicle controls: Water (H₂O) and Corn Oil (CO).
18
19
20
21
22
23
24
25
26
27
28
29
30
31
32
33
34
35
36
37

38 **Supplementary Figure S4. Proteomics analysis of phase II protein expression**
39 **in WT and CAR^h PXR^h mice.** Quantitative measurement of peptides using the *in*
40 *vivo* 'stable isotope labeling with amino acids in cell culture' (SILAC) technique from
41 (A) PB treated and (B) chlordane treated liver samples, in WT (filled bars) and in
42 CAR^h PXR^h (hatched bars) mice. Corresponding proteins are named on the X axis;
43 the Y axis is expressed in fold change expression, based of vehicle expression value.
44
45 Protein levels are indicated as mean ± SEM (H₂O and phenobarbital n=5 biological
46 replicates/group; CO and Chlordane n=3 biological replicates/group). Data were
47 analyzed using GraphPad Prism 7.0. Statistical significance of treated versus
48 untreated (vehicle) signal differences were tested using multiple unpaired t-tests on
49
50
51
52
53
54
55
56
57
58
59
60 36

1
2
3 log2 transformed data. The p-values were adjusted using Holm-Sidak method,
4
5 *p<0.05, **p<0.01, ***p<0.001, ****p<0.0001. Vehicle controls: Water (H₂O) and Corn
6
7 Oil (CO).
8
9

10 **Supplementary Figure S5. Role of *Dlk1-Dio3* non-coding RNAs in liver cancer**
11 **and their potential relevance as non-genotoxic carcinogenesis biomarkers. (A)**

12
13 The potential relevance of mechanisms of drug-induced tumors in humans is
14 frequently investigated by integrating tissue histopathology and biochemical and
15 molecular indicators of neoplastic risk. Mechanistic studies that integrate
16 phenotypically-anchored molecular and biochemical biomarkers have the potential to
17 provide mechanistic insights to help evaluate early on the risk for drug induced
18 carcinogenesis, as well as support the interpretation of drug-induced tumors and in
19 some cases provide valuable perspectives on potential relevance in humans (Moggs
20 et al. 2016). (B) Phenobarbital case study exemplifying the identification of *Dlk1-Dio3*
21 imprinted gene cluster noncoding RNAs as novel candidate biomarkers for
22 phenobarbital-induced liver tumor promotion (Lempiainen et al. 2013). Pathway
23 dependence (CAR and β -catenin) and phenotypic anchoring (e.g. tissue localization,
24 phenotype), represent important steps of the candidate biomarker characterization.
25
26 (C) Deregulation of the *Dlk1-Dio3* cluster was observed in numerous developmental
27 disorders and neoplasia, including hepatocellular carcinoma in humans and in mouse
28 models. *Dlk1-Dio3* associated non-coding RNA (including *Meg3*) genetically and
29 biochemically interact and regulate a number of important cellular processes whose
30 deregulation may be critical for tumor promotion and progression. snoRNA, small
31 nucleolus RNA.
32
33
34
35
36
37
38
39
40
41
42
43
44
45
46
47
48
49
50
51
52
53
54
55
56
57
58
59
60

Supplementary Table legends

Supplementary Table S1. List of model compounds and associated study designs. The compound class, known mechanism of action, link to CAR dependency and a summary of the *in vivo* experimental conditions are shown. GC: genotoxic carcinogenesis, NGC: non genotoxic carcinogenesis, CMC: carboxy-methyl cellulose, po: oral intake, ip: intraperitoneal injection.

Supplementary Table S2. List of selected xenobiotic metabolism genes, representing candidate CAR-activation dependent signature. The original study design contributing to the identification of the selected genes is indicated. po: oral intake, ip: intraperitoneal injection.

Supplementary Table S3. Microarray data of selected xenobiotic metabolism genes and *Dlk1-Dio3* cluster ncRNAs. The table indicates RMA-normalized and summarized by gene Log₂FC between treated and vehicle samples and adjusted p-values using the Benjamini-Hochberg method. The study ID indicates the key study and compound information. The drug, genetic background and time of treatment are indicated.

Tables

Table 1. Phenobarbital and chlordane lead to comparable liver phenotype *in vivo*. Toxicological and pathological data after 28 days (t=28) chlordane and 28 (t=28) or 91 (t=91) days PB treatment (Main) are shown. Recovery (Rec) was run for an additional 28 days for the chlordane and phenobarbital studies (t=56 and t=119 respectively). Body weight and plasma concentrations are indicated as mean value of indicated (n) individuals per group \pm standard deviation. *In vivo* data referring to the phenobarbital study are adapted from (Luisier et al. 2014). Centrilobular hypertrophy severity grades were on a 0-4 scale, expressed as median (n=5).

	phenobarbital									chlordane					
	wild - type			CAR ^h - PXR ^h			CAR ^{KO} - PXR ^{KO}			wild - type		CAR ^h - PXR ^h		CAR ^{KO} - PXR ^{KO}	
	Main t=28	Main t=91	Rec t=119	Main t=28	Main t=91	Rec T=119	Main t=28	Main t=91	Rec t=119	Main t=28	Rec t=56	Main t=28	Rec t=56	Main t=28	Rec t=56
Body weight	27.6 \pm 2.2 n=15	33.9 \pm 2.8 n=10	33.1 \pm 1.7 n=5	26.5 \pm 1.3 n=15	31.0 \pm 2.5 n=10	31.3 \pm 2.4 n=5	27.8 \pm 2.1 n=15	31.5 \pm 4.7 n=10	30.6 \pm 4.4 n=5	24.6 \pm 1.2 n=10	26.2 \pm 2.4 n=5	25.5 \pm 1.8 n=10	23.77 \pm 1.1 n=5	25.3 \pm 1.3 n=10	25.6 \pm 0.8 n=5
Plasma concentration (μ g/mL) n=5	19.7 \pm 3.6	11.1 \pm 3.2	0.0 \pm 0.0	32.3 \pm 5.2	17.0 \pm 7.2	0.0 \pm 0.0	82.7 \pm 8.9	52.6 \pm 6.3	0.0 \pm 0.0	7.7 \pm 3.5	1.0 \pm 0.4	4.8 \pm 1.2	2.3 \pm 2.0	5.2 \pm 2.0	2.1 \pm 1.3
Centrilobular hypertrophy (score 0:4) Median	2	3	2	3	3	1	0	1	0	3	2	3	2	0	0

1
2
3
4
5 Luisier, R., H. Lempiainen, N. Scherbichler, A. Braeuning, M. Geissler, V. Dubost, A. Muller, N. Scheer, S. D. Chibout, H. Hara, F.
6 Picard, D. Theil, P. Couttet, A. Vitobello, O. Grenet, B. Grasl-Kraupp, H. Ellinger-Ziegelbauer, J. P. Thomson, R. R. Meehan, C.
7 R. Elcombe, C. J. Henderson, C. R. Wolf, M. Schwarz, P. Moulin, R. Terranova, and J. G. Moggs. 2014. 'Phenobarbital induces
8 cell cycle transcriptional responses in mouse liver humanized for constitutive androstane and pregnane x receptors', *Toxicol*
9 *Sci*, 139: 501-11.
10
11
12
13
14
15
16
17
18
19
20
21
22
23
24
25
26
27
28
29
30
31
32
33
34
35
36
37
38
39
40
41
42
43
44
45
46
47
48
49

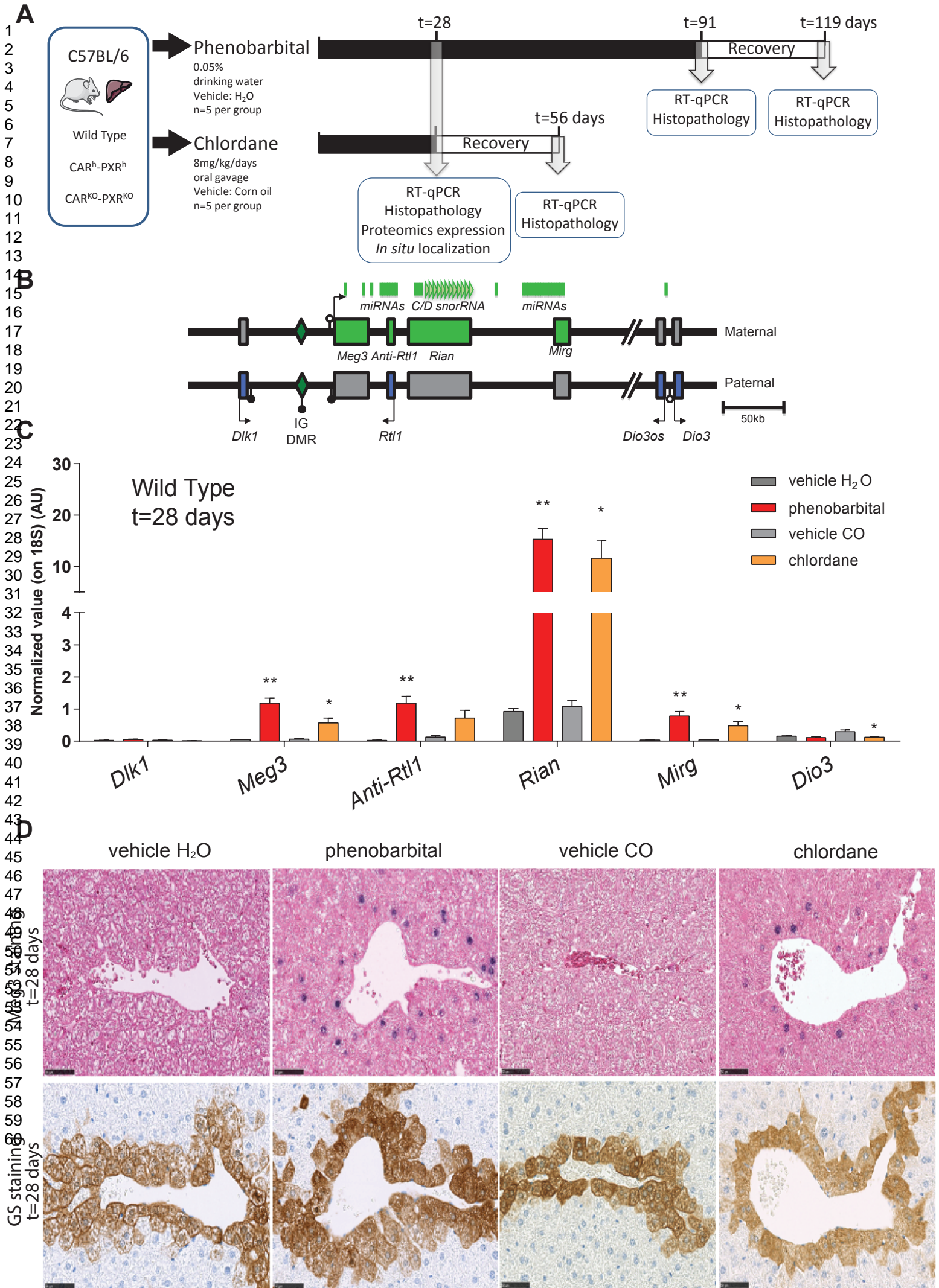
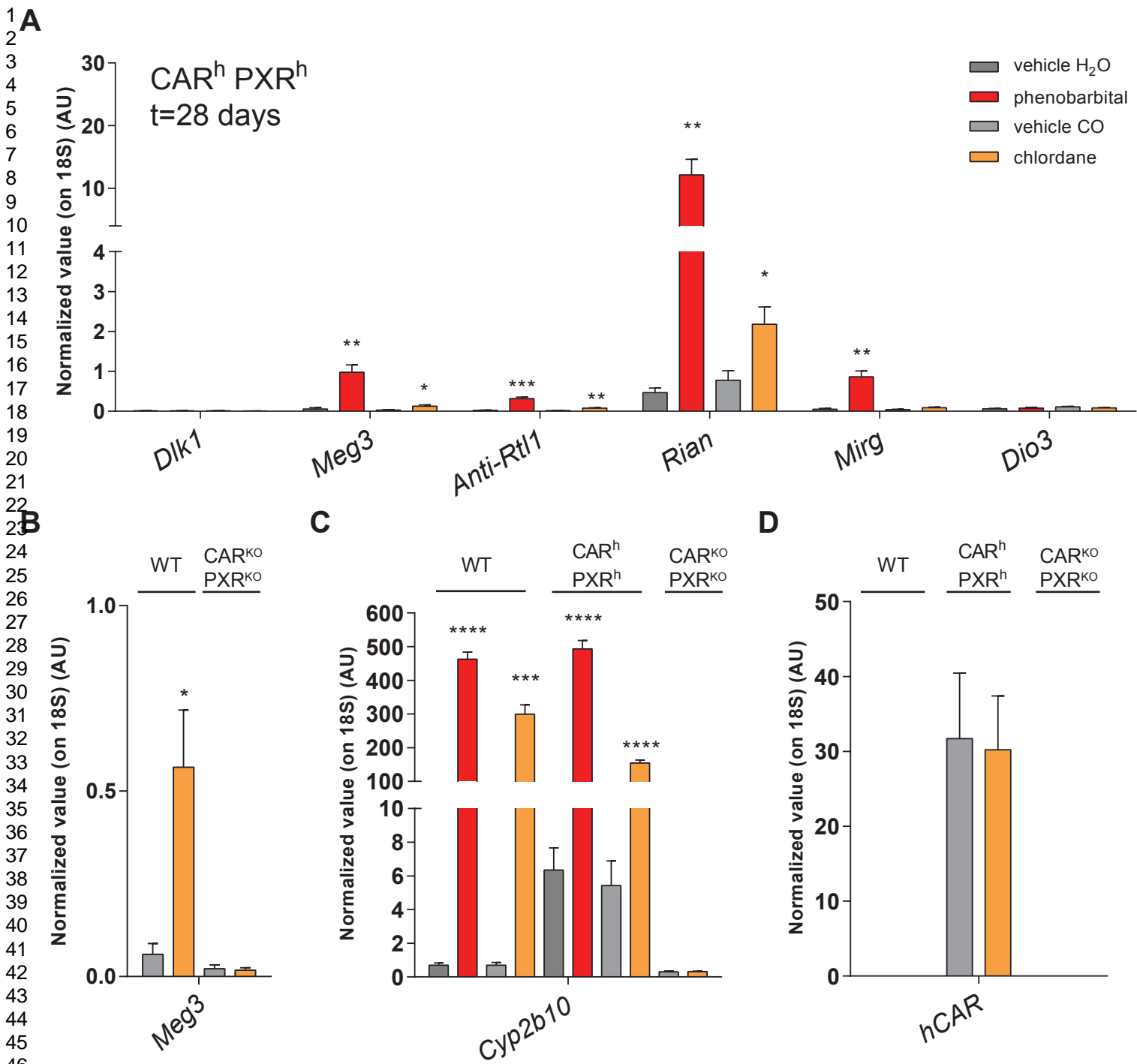
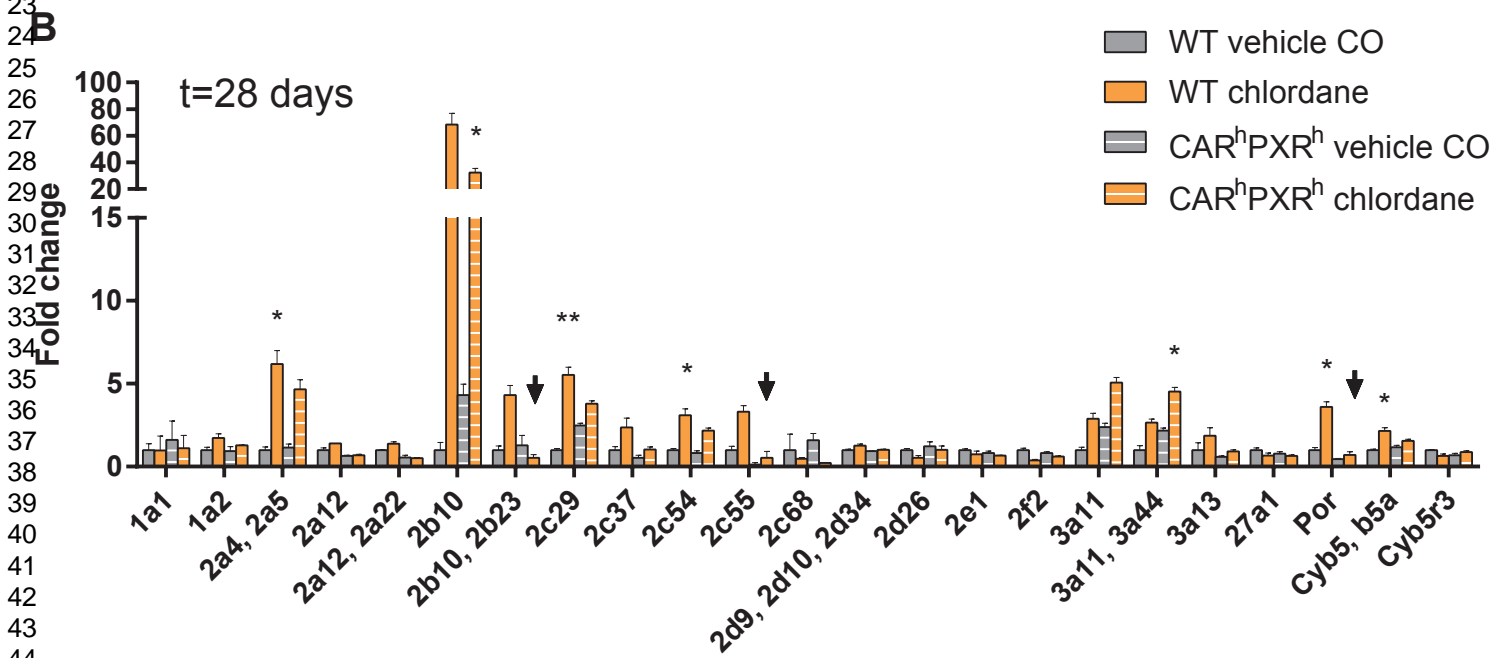
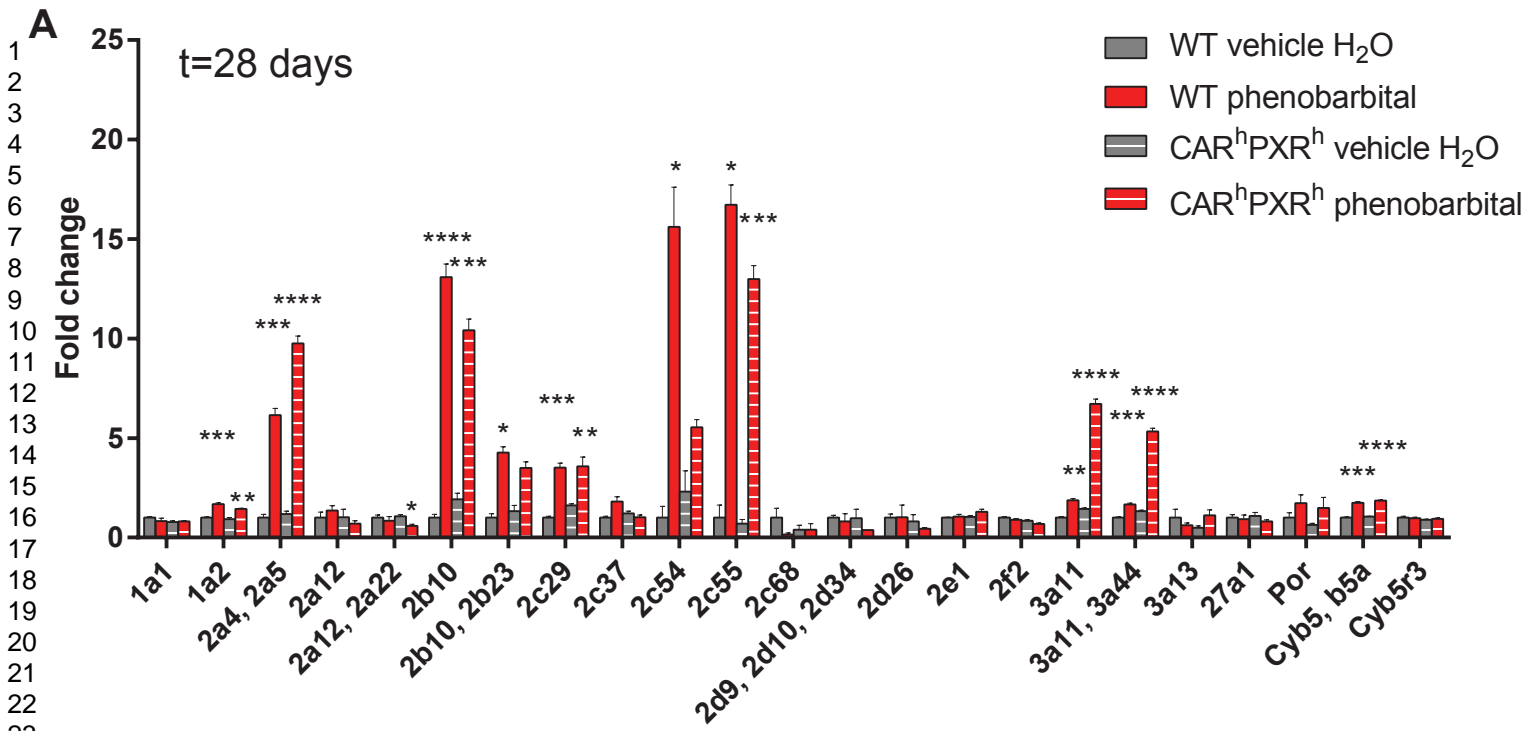


Figure 2. Pouché, Vitobello et al.



1
2
3
4
5
6
7
8
9
10
11
12
13
14
15
16
17
18
19
20
21
22
23
24
25
26
27
28
29
30
31
32
33
34
35
36
37
38
39
40
41
42
43
44
45
46
47
48
49
50
51
52
53
54
55
56
57
58
59
60



1
2
3
4
5
6
7
8
9
10
11
12
13
14
15
16
17
18
19
20
21
22
23
24
25
26
27
28
29
30
31
32
33
34
35
36
37
38
39
40
41
42
43
44
45
46
47
48
49
50
51
52
53
54
55
56
57
58
59
60

Cross species CAR activator

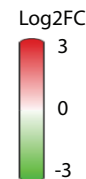
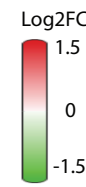
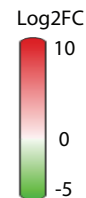
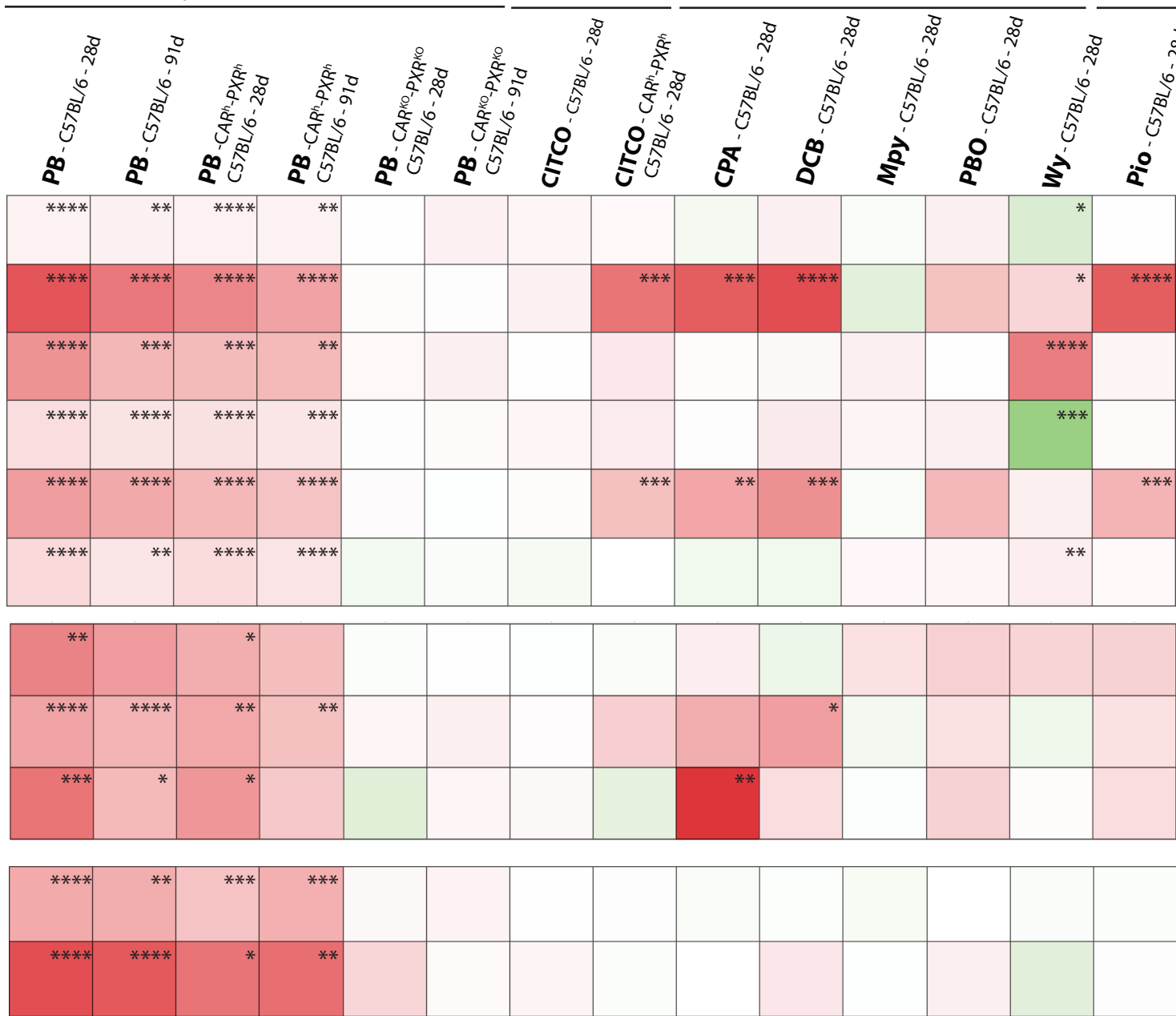
CAR activator

Liver NGC (other MoAs)

1
2
3
4
5
6
7
8
9
10
11
12
13
14
15
16
17
18
19
20
21
22
23
24
25
26
27
28
29
30
31
32
33
34
35
36
37
38
39
40
41

Xenobiotic response

Dlk1-Dio3 response



1
2
3
4
5
6
7
8
9
10
11
12
13
14
15
16
17
18
19
20
21
22
23
24
25
26
27
28
29
30
31
32
33
34
35
36
37
38
39
40
41
42
43

